Reaction Chemistry & Engineering

ROYAL SOCIETY OF CHEMISTRY

PAPER

View Article Online
View Journal

Cite this: DOI: 10.1039/d5re00547g

Kinetic insights into soybean peroxidase-catalyzed degradation of persistent organic pollutants

Alexandre Santuchi da Cunha, †[a] Monica Rigoletto, [b] Ardson dos Santos Vianna Jr. [a] and Enzo Laurenti *[b]

Received 7th December 2025,
Accepted 10th April 2026

DOI: 10.1039/d5re00547g

rsc.li/reaction-engineering

Soybean peroxidase (SBP)-catalysed degradation of 2,4,6-trichlorophenol (TCP), triclosan (TCS), and bisphenol A (BPA) was investigated in batch systems as single-substrate and multi-substrate reaction media representative of industrial effluents. SBP was extracted from soybean hulls, reactions were carried out in the presence of hydrogen peroxide as co-substrate and substrate depletion was monitored by HPLC. The experimental results showed that pollutant interactions in mixed systems significantly affect degradation kinetics, revealing limitations of conventional single-substrate descriptions. To capture these effects, a modified bi–bi ping-pong kinetic model was formulated and fitted to the experimental data by computational parameter estimation. The proposed multiple-substrate model successfully described competitive effects and simultaneous pollutant removal. The estimated kinetic constants indicated no substantial variation in k_1, associated with the reaction between the enzyme and hydrogen peroxide, whereas all the substrate-dependent constants reflected the competitive effects arising from the simultaneous presence of the three pollutants. These results provide mechanistic and quantitative insight into SBP-catalysed oxidation under realistic conditions and support the use of SBP-based kinetic frameworks for process optimization, enzyme engineering, and scale-up of enzymatic wastewater treatment technologies.

1. Introduction

Human activities often contribute to environmental degradation through the generation of various pollutants, including stable organic compounds such as pharmaceuticals, cosmetics and dyes, which are persistent and tend to accumulate in aquatic environments. Many different techniques have been proposed for pollutants' removal, each with its own strengths and weaknesses.[1]

Among them, advanced oxidation processes (AOPs) are among the most promising ones commonly used to treat these effluents.[2,3] However, their large-scale implementation remains limited. Enzymes have therefore emerged as a potential alternative to these chemical methods due to their specificity in catalyzing degradation reactions of such compounds.[4–6]

Among the various remediation strategies, enzyme-based oxidation processes have gained increasing attention because of their high selectivity, operation under mild conditions, and reduced formation of secondary pollutants when compared to conventional advanced oxidation processes.[3–6] Within this context, soybean peroxidase (SBP) is particularly interesting because it can be sustainably extracted from soybean hulls, an abundant agro-industrial residue,[6–8] and has shown effective catalytic performance toward phenolic and chlorinated compounds in previous studies.[7,8] SBP also exhibits good operational stability over a relatively broad range of conditions, which supports its relevance for mechanistic and reaction engineering studies.[4,6,9–12] However, as with AOPs, the scale-up of enzymatic systems remains limited by factors such as enzyme cost, inactivation, recovery, and the complexity of real wastewater matrices. These advantages and limitations must therefore be considered together when evaluating SBP as a candidate for treatment technologies.[6–8]

In many industrial and urban effluents, pollutants such as triclosan (5-chloro-2-(2,4-dichlorophenoxy)phenol, TCS), 2,4,6-trichlorophenol (TCP), and bisphenol A (4,4′-(propane-2,2-diyl) diphenol, BPA) are recalcitrant to common environmental degradation processes, remaining persistent. These substances are known to cause several health problems.[13–15] However, the products resulting from enzymatic treatment are usually less toxic than the parent compounds.[16] Thus, the use of SBP can be a promising and eco-friendly method for remediating industrial effluents.[6–8,16]

[a] Departamento de Engenharia Química, Escola Politécnica, Universidade de São Paulo, São Paulo, Brazil
[b] Dipartimento di Chimica, Università Degli Studi di Torino, Torino, Italy. E-mail: enzo.laurenti@unito.it
† Present address: Escola de Engenharia, Universidade Presbiteriana Mackenzie, São Paulo, Brazil.

TCP is a priority pollutant frequently detected in industrial effluents and freshwater environments, and its enzymatic degradation by peroxidases has been extensively investigated.[13,17] Torres and Ayala (2010)[18] demonstrated TCP degradation through two one-electron oxidations mediated by peroxidase. Ferrari *et al.* (1999)[19] proposed a catalytic mechanism for TCP oxidative dechlorination involving horseradish peroxidase (HRP) and H_2O_2, leading to the formation of chlorinated quinones, while Laurenti *et al.* (2002, 2003)[20,21] confirmed related pathways using spectroscopic techniques.

TCS is a fungicidal and bactericidal agent widely used in personal care products and frequently detected in water bodies.[14,22] Literature reports have examined TCS degradation using different oxidative enzymes, including laccases, manganese peroxidase, HRP, and SBP.[22,23] While degradation mechanisms and products have been proposed for laccase-catalysed reactions,[22,24] mechanistic information for peroxidase-mediated TCS degradation remains limited. Li *et al.* (2016)[14] identified the formation of dimers and trimers as major products of the SBP-catalysed reaction, indicating the need for further investigation.

BPA is a synthetic organic compound commonly detected in surface waters and wastewater[25] and is suspected to act as an endocrine-disrupting compound.[26] Numerous studies have investigated BPA degradation using peroxidases, particularly HRP.[15,25–28] Kobayashi (1998)[29] reported oxidative polymerization of BPA catalysed by SBP and HRP, while Huang and Weber (2005)[27] proposed detailed degradation mechanisms involving multiple intermediates identified by chromatographic and spectrometric techniques.

Therefore, the study of the degradation of TCP, TCS, and BPA represents a relevant model for industrial effluents, especially when these pollutants are present simultaneously, since competitive interactions between substrates may occur.[30–32]

Previous studies have also investigated fundamental aspects of SBP catalysis and intermediate formation,[4,9–11,33] providing insight into enzyme reactivity, stability, and limitations. In addition, reviews of SBP applications in wastewater treatment have highlighted both advances and remaining challenges, including enzyme cost, recycling strategies, and the limited number of studies conducted with real effluents.[6]

Several studies have demonstrated that the presence of multiple substrates can significantly influence degradation kinetics.[30–32] Regarding the modeling of enzymatic reactions, classical and modern kinetic frameworks have been developed to describe peroxidase-catalyzed processes.[34–42] However, most modeling studies remain focused on single-substrate systems or simplified reaction media, limiting their applicability to complex effluents and competitive degradation scenarios.[30–32,43–45]

Previous kinetic studies on the enzymatic removal of phenolic and chlorophenolic pollutants using SBP and HRP have been conducted in a variety of reactor configurations, highlighting the strong influence of reactor type on apparent kinetics and process performance. Gómez *et al.* (2008)[43] employed a continuous stirred-tank reactor (CSTR) to investigate the removal of 4-chlorophenol using SBP and H_2O_2, demonstrating that a simplified steady-state reactor model based on a bi–bi ping-pong kinetic mechanism could successfully predict experimental conversions under ideal mixing conditions. In a subsequent study, Gómez Carrasco *et al.* (2011)[44] developed a diffusion–reaction kinetic model for phenolic compound removal using immobilized peroxidase in particulate catalysts, explicitly accounting for enzyme deactivation caused by polymeric film formation and internal diffusion limitations; the model was validated using batch reactor experiments and proved capable of reproducing system behaviour across multiple operating conditions. More recently, da Cunha *et al.* (2021)[45] investigated the degradation of 2,4,6-trichlorophenol by SBP in a microreactor, comparing multiple bi–bi ping-pong kinetic formulations and demonstrating that inclusion of all enzyme intermediate forms and inactivation pathways significantly improved model accuracy, enabling more reliable reactor design and process simulation. While these studies collectively demonstrate the applicability of peroxidase-based kinetics across continuous, batch, immobilized, and microreactor systems, most analyses remain focused on single-substrate conditions. Kinetic descriptions capable of capturing competitive effects in multi-substrate reaction media representative of real effluents are still scarce, motivating the present study.

The toxicity of transformation products formed during SBP-catalysed degradation of TCP, TCS, and BPA was previously investigated by Rigoletto *et al.* (2023)[12] using enzymatic systems based on soybean peroxidase. In that study, the combined effects of pollutant removal and toxicity reduction were systematically evaluated, demonstrating that enzymatic treatment led to a significant decrease in overall toxicity of treated water matrices. Building upon these findings, the present work focuses on the kinetic and mechanistic aspects of SBP-catalysed degradation, aiming to quantitatively describe single- and multi-substrate reaction systems and to provide reaction engineering tools for process design and scale-up.

2. Materials and methods

Currently, SBP is not commercially available, so it was extracted, purified, and used in experiments to evaluate its catalytic efficiency in degrading TCP, TCS, and BPA. These degradation experiments were conducted in a batch reactor setup to monitor the reaction progress under reproducible and clearly defined conditions, ensuring proper control of temperature, pH, and reagent concentrations.

To develop a comprehensive and quantitative understanding of the degradation process catalyzed by SBP, it is crucial to employ a robust mathematical framework that accurately describes the reaction kinetics. Accordingly, a modified version of the bi–bi ping pong kinetic model was proposed to account for the complex interactions between the enzyme, substrates,

and H_2O_2. This model serves as a foundation for capturing the dynamics of both single and multi-substrate systems.

Using experimental data, several key kinetic parameters were estimated through nonlinear regression techniques, implemented in MATLAB. These parameters provide critical insights into the catalytic behavior of SBP.

2.1 Soybean peroxidase extraction and purification

SBP enzyme was extracted from soybean hulls following the procedure carried out by Calza *et al.* (2016)[7] and Tolardo *et al.* (2019):[8] soybeans hulls are manually removed from seeds and proteins are extracted by treatment with phosphate buffer 0,1 M at pH 7; the mixture was centrifuged to separate the hulls, and the supernatant is tested for peroxidase activity. The SBP-containing solution undergoes concentration, protein precipitation using ammonium sulphate, dialysis, and ion exchange chromatography to obtain the final purified SBP sample which is stored at −12 °C. The enzyme's activity is assessed using the Ngo and Lenhoff (1980)[46] method, involving a colorimetric spectrophotometric assay based on the oxidative coupling of 3-(dimethylamino)benzoic acid (DMAB) and 3-methyl-2-benzothiazolinonehydrazone (MBTH) in the presence of H_2O_2. The kinetics of the formation of the dark purple product are followed by measuring the absorbance at 590 nm over time.

Enzyme concentration was calculated from the maximum absorbance of the Soret band at 403 nm (typical for the Fe(III)-heme group in HRP and SBP) by a double-beam Unicam UV300 spectrophotometer. SBP enzyme has a molar absorptivity at 403 nm of 94 600 M^{-1} cm^{-1}.[47] Considering a pathlength (L) of 1 cm, the enzyme concentration can be calculated using the following (eqn (1) and (2)):

$$\varepsilon_{403\text{nm}} = \frac{\text{Abs}_{403\text{nm}}}{[\text{Enzyme}] \times L} \quad (1)$$

$$[\text{Enzyme}] = \frac{\text{Abs}_{403\text{nm}}}{\varepsilon_{403\text{nm}} \times L} \quad (2)$$

2.2 Enzymatic reactions

After obtaining the purified SBP, experiments are performed in batch mode, to carry out the reactions in a scenario closer to a practical application. In this case, the process represents a global kinetics, where mass transfer is also considered. The behavior of SBP in a medium with multiple organic substrates, composed of TCP, TCS, and BPA, is evaluated and the degradation is compared to that obtained in single-substrate solutions. All enzymatic batch reactions are conducted in a beaker with constant magnetic stirring, in a total reaction volume of 10 mL. Volumes of 10 μL are collected at fixed times and analyzed in a Merck-Hitachi HPLC equipped with a LiChrospher RP-C18 reverse phase column (5 μm, 4 mm i.d. × 125 mm long, Merck) and a Hitachi L-4200 UV-visible detector. Elution is carried out with acetonitrile and phosphate buffer (1×10^{-2} M, pH 2.8) (70 : 30% v/v) at a flow rate of 1 mL min^{-1} and the analytical detector wavelength is set at 242 nm. This single detection wavelength was selected to enable simultaneous monitoring and quantitative comparison of TCP, TCS, and BPA within the same analytical method. The sampling volume was chosen so that the variation in the total reaction volume is not significant.

For each substrate, a 1000 mg L^{-1} stock solution in acetonitrile is prepared, to avoid problems with the solubility of the compounds in water. The final solutions are prepared by diluting the stock solution in MilliQ water up to a concentration of 5 mg L^{-1} and with a final content of acetonitrile below 0.5%, which does not affect the enzyme activity.[24] The reactions are carried out considering fixed contaminants concentrations of 5 and 15 mg L^{-1}, 0.1 mM of H_2O_2, and three enzyme concentrations (4.39×10^{-9} M, 8.77×10^{-9} M, and 1.75×10^{-8} M).

Calibration curves are obtained for TCP, TCS, and BPA, by preparing solutions of different concentrations in MilliQ water, analyzing them in the HPLC system, and correlating the characteristic peak areas with their corresponding concentrations. Although SBP was used in soluble form, no interference with HPLC analysis was observed, as the enzyme was present at nanomolar concentrations, did not interact with the reversed-phase column, and did not absorb at the analytical detection wavelength used for pollutant quantification.

2.3 Rationale for substrate selection and kinetic approach

The kinetic characterization of SBP requires the use of phenolic substrates that act as both mechanistic probes and environmentally relevant model compounds. Phenolic and chlorinated phenolic compounds are well-established substrates for peroxidase-catalysed oxidation, as their degradation can proceed *via* one-electron transfer reactions mediated by the formation of enzyme intermediates (compounds I and II). Consequently, such substrates are routinely employed to elucidate peroxidase reaction mechanisms and to quantify kinetic parameters relevant to reactor design.

In this study, TCP, TCS, and BPA were selected to represent structurally distinct phenolic pollutants commonly detected in industrial and urban effluents. TCP is a chlorinated phenol with high electron-withdrawing substitution, TCS is a polyhalogenated phenoxyphenol, and BPA is a non-halogenated bisphenol compound. Together, these substrates provide a representative spectrum of reactivity, steric effects, and electronic properties relevant to SBP-catalysed oxidation.

While single-substrate experiments allow the estimation of intrinsic kinetic parameters, real effluents typically contain multiple phenolic contaminants that compete for the enzyme active site. For this reason, both single- and multi-substrate experiments were performed. The latter are essential to capture competitive effects and interaction phenomena that cannot be described by simplified kinetic models. This experimental strategy directly motivates the use of a modified bi–bi ping-

pong kinetic framework, which enables quantitative description of simultaneous substrate degradation under conditions relevant to engineering applications.

2.4 Single substrate model

The peroxidase reactions follow a bi–bi Ping-Pong mechanism, which is the same approach previously described by Costa *et al.* (2020)[48] and da Cunha *et al.* (2021).[45] This process involves the transfer of two electrons to the first substrate (H_2O_2), creating a first oxidized enzyme intermediate called 'Compound I' (CpI), followed by two successive one-electron oxidations of the second substrate (S) to return the enzyme to its reduced state *via* a second enzyme intermediate called 'Compound II' (CpII).[5,36] It is important to note that peroxidase can be deactivated if there is too much H_2O_2, which generates a third enzyme oxidized intermediate called 'Compound III' (CpIII). However, in this work, only the model with CpI and CpII formation was considered (Fig. 1, black pathway).

The process modeling was obtained from the mass balance of all the species of the schematic reactions as described by Costa *et al.* (2020)[48] and da Cunha *et al.* (2021).[45] The system of differential equations is presented in eqn (3) to (8):

$$\frac{d[E]}{dt} = -k_1[E][H_2O_2] + k_3[CpII][S] \quad (3)$$

$$\frac{d[CpI]}{dt} = k_1[E][H_2O_2] - k_2[CpI][S] \quad (4)$$

$$\frac{d[CpII]}{dt} = k_2[CpI][S] - k_3[CpII][S] \quad (5)$$

$$\frac{d[H_2O_2]}{dt} = -k_1[E][H_2O_2] \quad (6)$$

$$\frac{d[S]}{dt} = -k_2[CpI][S] - k_3[CpII][S] \quad (7)$$

$$\frac{d[P]}{dt} = k_2[CpI][S] + k_3[CpII][S] \quad (8)$$

A steady state can be assumed for all forms of the enzyme as equilibria are quickly reached because of fast reactions (eqn (9)):

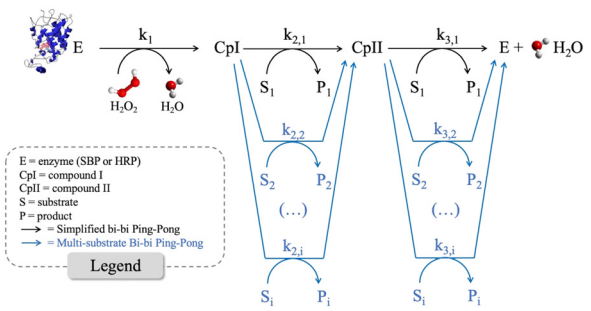

Fig. 1 Scheme of the bi–bi ping-pong reaction mechanism. In blue, the mechanism proposed for a multi substrate model.

$$\frac{d[E]}{dt} = \frac{d[CpI]}{dt} = \frac{d[CpII]}{dt} = 0 \quad (9)$$

The total (initial) amount of enzyme, $[E]_0$, is given by eqn (10), and as this value is known, $[E]$ can be obtained (eqn (10)):

$$[E]_0 = [E] + [CpI] + [CpII] \quad (10)$$

From eqn (4), (5), and (9), the concentrations of CpI and CpII can be calculated. In this way, a system of algebraic-differential equations (DAE) is obtained, consisting of (eqn (11)–(16)):

$$[E] = [E]_0 - [CpI] - [CpII] \quad (11)$$

$$[CpI] = \frac{k_1[E][H_2O_2]}{k_2[S]} \quad (12)$$

$$[CpII] = \frac{k_2[CpI]}{k_3} \quad (13)$$

$$\frac{d[H_2O_2]}{dt} = -k_1[E][H_2O_2] \quad (14)$$

$$\frac{d[S]}{dt} = -k_2[CpI][S] - k_3[CpII][S] \quad (15)$$

$$\frac{d[P]}{dt} = k_2[CpI][S] + k_3[CpII][S] \quad (16)$$

2.5 Multi substrate model

A more complex model represented on Fig. 1 (blue pathway) is being proposed in this research considering the degradation of a multi-substrate solution, based on the fundamentals presented by Costa *et al.* (2020)[48] and da Cunha *et al.* (2021)[45] and the equations presented in the previous section. Because of the higher number of variables involved in this case, the simplest model can be assumed, considering only the CpI and CpII intermediates.

Assuming that all substrates interact equally with the enzyme forms, the reactions can be represented by eqn (17) and (18):

$$CpI + S_i \xrightarrow{k_{2i}} CpII + P_i \quad (17)$$

$$CpII + S_i \xrightarrow{k_{3i}} E + H_2O + P_i \quad (18)$$

In these reactions, S_i and P_i refer to each substrate and its respective product, and k_{2i} and k_{3i} are their relative kinetic constants. Then, it's possible to obtain the ordinary differential equation (ODE) system generated by the model – eqn (19)–(24):

$$\frac{d[E]}{dt} = -k_1[E][H_2O_2] + \sum_{i=1}^{n} k_{3i}[CpII][S_i] \quad (19)$$

$$\frac{d[CpI]}{dt} = k_1[E][H_2O_2] - \sum_{i=1}^{n} k_{2i}[CpI][S_i] \quad (20)$$

$$\frac{d[CpII]}{dt} = \sum_{i=1}^{n} k_{2i}[CpI][S_i] - \sum_{i=1}^{n} k_{3i}[CpII][S_i] \quad (21)$$

$$\frac{d[H_2O_2]}{dt} = -k_1[E][H_2O_2] \quad (22)$$

$$\frac{d[S_i]}{dt} = -\sum_{i=1}^{n} k_{2i}[CpI][S_i] - \sum_{i=1}^{n} k_{3i}[CpII][S_i] \quad (23)$$

$$\frac{d[P_i]}{dt} = \sum_{i=1}^{n} k_{2i}[CpI][S_i] + \sum_{i=1}^{n} k_{3i}[CpII][S_i] \quad (24)$$

The DAE system can also be obtained in this case, also considering the total (initial) amount of enzyme and assuming steady-state conditions for the concentrations of all enzyme forms (eqn (25)–(30)):

$$[E] = [E]_0 - [CpI] - [CpII] \quad (25)$$

$$[CpI] = \frac{k_1[E][H_2O_2]}{\sum_{i=1}^{n} k_{2i}[S_i]} \quad (26)$$

$$[CpII] = \frac{\sum_{i=1}^{n} k_{2i}[CpI][S_i]}{\sum_{i=1}^{n} k_{3i}[S_i]} \quad (27)$$

$$\frac{d[H_2O_2]}{dt} = -k_1[E][H_2O_2] \quad (28)$$

$$\frac{d[S_i]}{dt} = -\sum_{i=1}^{n} k_{2i}[CpI][S_i] - \sum_{i=1}^{n} k_{3i}[CpII][S_i] \quad (29)$$

$$\frac{d[P_i]}{dt} = \sum_{i=1}^{n} k_{2i}[CpI][S_i] + \sum_{i=1}^{n} k_{3i}[CpII][S_i] \quad (30)$$

2.6 Model validation and parameter estimation procedures

The initial guesses for obtaining the kinetic constants in the model simulation and parameter estimation procedures are taken from the kinetic constants reported in the literature listed in Table 1. These reaction rate constants were reported by Nicell (1994)[36] and Nicell and Wright (1997)[37] after reviewing previous works of different authors. The constants were obtained for the HRP enzyme with the substrate 4-chlorophenol at 25 °C and pH 7. The other kinetic constants are generally obtained from the HRP enzyme and its modified forms with H_2O_2 as substrate. It should be noted that, although the SBP and HRP enzymes are structurally and functionally similar, the different behavior of these enzymes cannot be excluded without experimental evidence.

Table 1 Reaction constants used in the model development. Adapted from ref. 36 and 37

Constant	Value (M^{-1} s^{-1})
k_1	2.0×10^7
k_2	1.13×10^7
k_3	1.1×10^6

The procedure for estimating parameters was carried out by using MATLAB software version R2015a and it is illustrated in Fig. 2. It involves a main routine that reads all experimental data and solves the optimization problem using the *fmincon* optimizer with the interior point method, and tolerances of 10^{-10}. The model solution is then carried out by the backward differentiation formula (BDF) method, using the *ode15s* solver implemented in MATLAB. Relative and absolute tolerances of 10^{-8} and 10^{-10}, respectively, are considered. The default settings are applied to all other methods. The initial estimates of kinetic constants are obtained from the values presented in Table 1. Additionally, the kinetic constants are reparametrized using the natural logarithm of the values to ensure that only positive values are used. This is important as positive values have real physical meaning in this case, indicating that the kinetic constants are positive numbers.

The objective function (OF) is minimized using the weighted least squares function obtained from the maximum likelihood method.[49] This function considers the predicted values (u) calculated by the model and their respective experimental data set (u_i) for a certain number of points (n) and experiments (m). Eqn 31 depicts this relationship.

Additionally, this equation considers the standard deviation of the experimental data (σ) calculated for each set of experiments using eqn (32). Here, u_i represents the average of the experimental data.[45]

$$OF = \min \sum_{j=1}^{m} \sum_{i=1}^{n} \frac{(\hat{u}_{ij} - u_{ij})^2}{2\sigma_{ij}^2} \quad (31)$$

$$\sigma = \sqrt{\frac{\sum_{i=1}^{n} (u_{ij} - \overline{u}_{ij})^2}{n}} \quad (32)$$

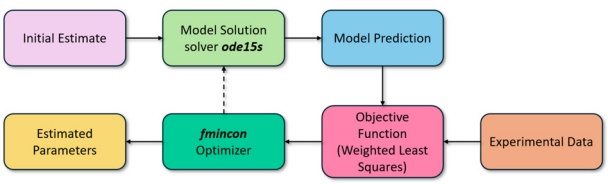

Fig. 2 Flowchart of the parameter estimation procedure implemented in MATLAB R2015a.

The fit of the model is assessed by comparing the plots of the model predictions with the experimental data. The evaluation is done by calculating the root mean squared error (RMSE) and the adjusted coefficient of determination (R^2) using the formulas given in eqn (33) and (34). Here, p denotes the number of parameters.

$$\mathrm{RMSE} = \sqrt{\sum_{i=1}^{n} \frac{(\hat{u}_i - u_i)^2}{n}} \tag{33}$$

$$R^2_{\mathrm{adjusted}} = 1 - \frac{(1-R^2)(n-1)}{n-(p+1)} \tag{34}$$

$$R^2 = 1 - \frac{\sum_{i=1}^{n} (\hat{u}_i - u_i)^2}{\sum_{i=1}^{n} (\hat{u}_i - \bar{u}_i)^2} \tag{35}$$

When evaluating a regression model, it is important to consider both the RMSE and the adjusted R^2. The RMSE should be as small as possible, while the adjusted R^2 should be as high as possible. The reason why an adjusted R^2 is preferred over R^2 is that it considers the penalty for including additional parameters that do not contribute to the model's fit. This means that adjusted R^2 is a better tool for comparing and evaluating different models. However, it is important to keep in mind that adjusted R^2 is not always reliable for non-linear models, so other criteria should be used in conjunction with it. Finally, the quality of the model fit can be assessed by examining the value of the OF (objective function) for each case. A smaller value of OF indicates a better minimization of the OF and, consequently, a better result in the optimization process.

3. Results and discussion

3.1 Soybean peroxidase extraction and purification

The enzyme SBP was obtained successfully from soybean seed hulls after carrying out the procedure described in section 2.1. The activity test and spectroscopic analysis of the extracted enzyme confirmed the presence of the SBP enzyme in the product obtained. The activity graphs obtained by the spectrophotometric analysis are shown in Fig. 3.

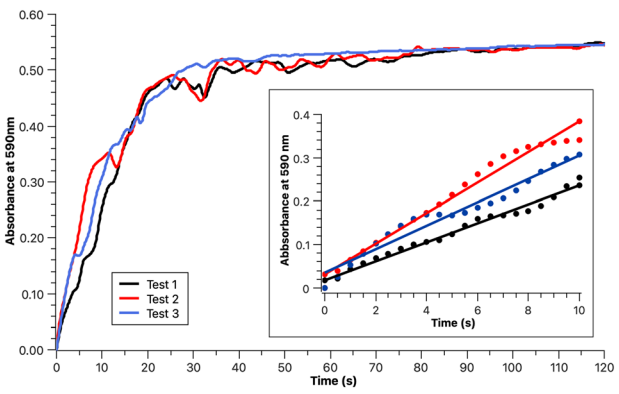

Fig. 3 Activity test of purified SBP (inset: data used for initial rate calculation of the specific activity).

Considering the average of the slopes, an activity of 35 μmol min^{-1} was obtained. From the spectroscopic analysis, the maximum absorbance at 403 nm obtained was 0.335. According to eqn (2) and considering the dilution factor of 1 : 25, the calculated SBP concentration was 8.85 × 10^{-5} M. This solution is then diluted in MilliQ water to obtain the desired concentrations (4.39 × 10^{-9} M, 8.77 × 10^{-9} M, and 1.75 × 10^{-8} M).

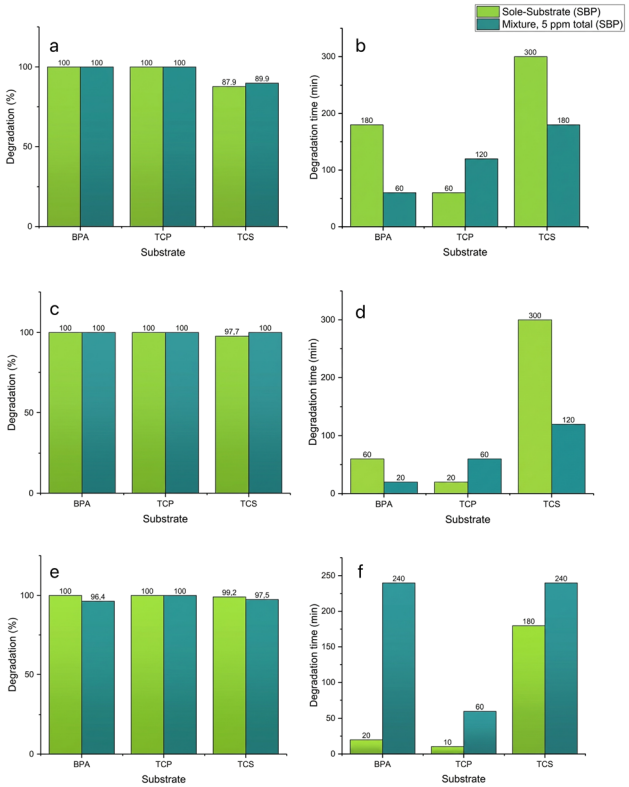

Fig. 4 Summary of the degradation results obtained in single and multi-substrate experiments obtained with a) and b) [SBP] =4.39 × 10^{-9} M; c) and d) 8.77 × 10^{-9} M, and e) and f) 1.75 × 10^{-8} M.

3.2 Enzymatic batch reactions

Batch experiments were conducted to investigate enzymatic degradation reactions in a scenario that closely resembles an

Table 2 Estimated parameters and model fit evaluation for single-substrate degradation

Parameter	TCP	BPA	TCS	Unit
k_1	2.0 × 10^7	2.0 × 10^7	2.0 × 10^7	M^{-1} s^{-1}
k_2	2.98 × 10^6	3.81 × 10^6	1.60 × 10^6	M^{-1} s^{-1}
k_3	2.26 × 10^5	4.21 × 10^5	3.20 × 10^4	M^{-1} s^{-1}
OF	3.2512 × 10^{-2}	3.8340 × 10^{-2}	1.6043 × 10^{-1}	—
RMSE	8.31 × 10^{-12}	4.37 × 10^{-12}	9.03 × 10^{-12}	—
$R^2_{\mathrm{adjusted},1}$	99.81%	93.25%	64.65%	—
$R^2_{\mathrm{adjusted},2}$	96.86%	97.96%	96.01%	—
$R^2_{\mathrm{adjusted},3}$	94.98%	99.85%	97.61%	—

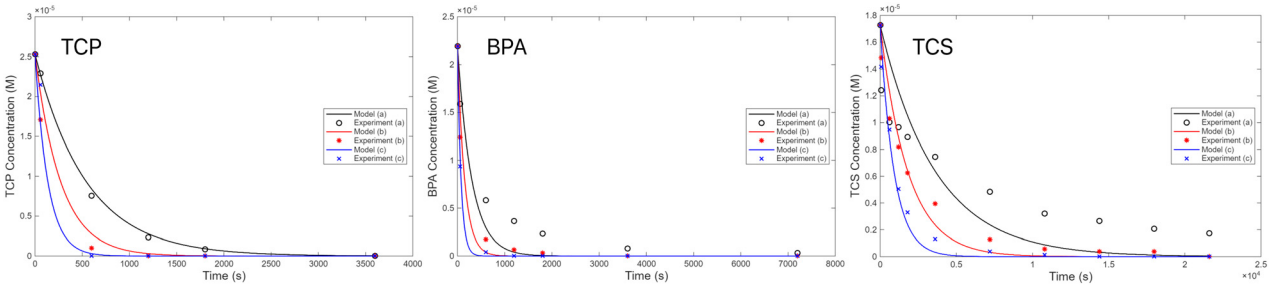

Fig. 5 Model prediction and experimental data of single-substrate degradation in batch of TCP (I), BPA (II) and TCS (III). SBP concentrations are a) 4.39×10^{-9} M, b) 8.77×10^{-9} M, and c) 1.75×10^{-8} M. Model quality was evaluated using adjusted R^2, RMSE, and objective function (OF) values reported in Table 2.

Table 3 Simulation considering single-substrate degradation model and multi-substrate degradation data

Parameter	TCP	BPA	TCS	Unit
k_1	2.0×10^7	2.0×10^7	2.0×10^7	$M^{-1}\ s^{-1}$
k_2	2.98×10^6	3.81×10^6	1.60×10^6	$M^{-1}\ s^{-1}$
k_3	2.26×10^5	4.21×10^5	3.20×10^4	$M^{-1}\ s^{-1}$
RMSE	9.08×10^{-12}	1.77×10^{-12}	5.04×10^{-12}	—
$R^2_{\text{adjusted},1}$	80.56%	95.24%	65.80%	—
$R^2_{\text{adjusted},2}$	91.86%	99.78%	55.48%	—
$R^2_{\text{adjusted},3}$	91.69%	96.70%	92.60%	—

industrial application. The study aimed to analyze the degradation of pollutants such as TCP, TCS, and BPA using SBP. The analyses included single-substrate degradation *versus* multi-substrate degradation. In this study, the reactions were carried out globally, considering transport and mixing processes. All data presented in this study are based on a batch process that is closer to a real-world scenario.

TCP, TCS, and BPA were identified by HPLC at retention times of approximately 2.77–2.79, 4.42–4.44, and 1.58–1.60 minutes, respectively. The calibration curves exhibited excellent linearity over the concentration ranges investigated, with coefficients of determination (R^2) of 99.83% for TCP, 99.84% for TCS, and 99.5% for BPA.

Prior to HPLC analysis, aliquots were directly injected (no filtration step), and no column fouling or backpressure increase was observed throughout the experiments, indicating that any transient oligomeric products did not interfere with chromatographic operation under the conditions employed.

In TCP degradation reactions, it was possible to observe the formation of two products, at the retention times of 1.25–1.28 and 1.83–1.84 minutes, respectively. Although it is not possible to identify these reaction products through the HPLC-UV technique used, this result seems to be consistent with a previous study,[19] where the authors identified 2,6-dichloro-1,4-benzoquinone and 2,6-dichlorohydroquinone as the two products obtained from oxidative dechlorination of TCP in the presence of HRP and H_2O_2.

For BPA, it was not possible to observe the reaction products, probably because the wavelength chosen for HPLC-UV analysis was not the most suitable for these specific compounds, or even because it is well known that during the reaction a mixture of higher-molecular-weight products is formed, starting from the first radical intermediate.[12,27]

Regarding the reaction products of TCS, it was possible to observe a major product at a retention time of 1.21–1.25 minutes, and several products at retention times ranging from 0.58 seconds to 3.97 minutes which appear in the first reaction stage and successively undergo enzymatic transformation and disappear. Indeed, according to the literature,[22,24] TCS products are different dimers, trimers, and oligomers, as for BPA. So, this result is consistent with what was predicted in the literature.

The study performed degradation reactions of TCP, BPA, and TCS in batch reactors, both individually and in a mixture, to emulate effluents that can contain multiple components as potential pollutants. For enzyme concentrations of 4.39×10^{-9} M and 8.77×10^{-9} M, the reaction medium had a total substrate concentration of 5 ppm, while for an enzyme concentration of 1.75×10^{-8} M, a total substrate concentration of 15 ppm was used, with equal amounts of substrates in both cases. Fig. 4 presents a comparison between the single-substrate degradation with SBP and the degradation in multi-substrate media with SBP, showing that a substrate's behavior may vary depending on the situation.

First, the degradation of individual pollutants in a mixture with the SBP enzyme can be compared. As shown in Fig. 4(a) and (c), the degradation of BPA was observed to be complete in single-substrate degradation as well as in a mixture with SBP enzyme concentrations of 4.39×10^{-9} M and 8.77×10^{-9} M. However, the degradation was faster in the mixture for these SBP concentrations (Fig. 4(b)). At an SBP concentration of 1.75×10^{-8} M, the behavior was opposite, with complete and much faster degradation in the case of single-substrate degradation (Fig. 4(e) and (f)).

TCP showed complete degradation for both single-substrate degradation and degradation in a mixture with SBP for all enzyme concentrations. The degradation was faster in the case of single-substrate degradation (Fig. 4(b), (d) and (f)), in contrast to BPA for lower enzyme concentrations.

TCS degraded better in the mixture for SBP concentrations of 4.39×10^{-9} M and 8.77×10^{-9} M and presented better

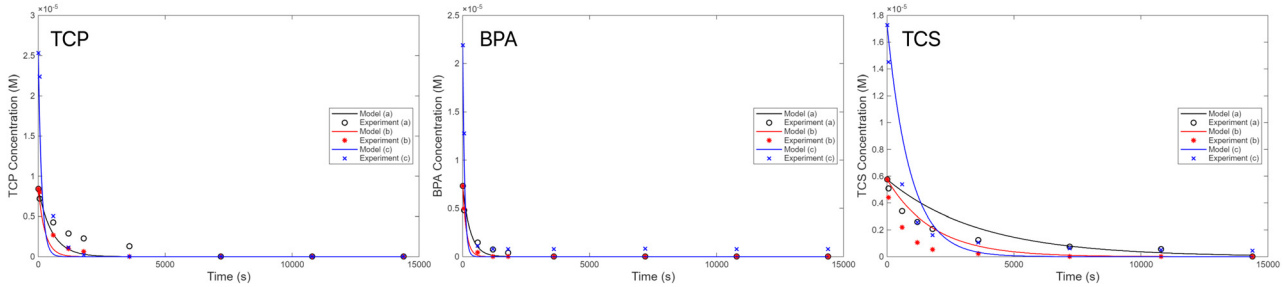

Fig. 6 Model simulation and experimental data of single-substrate degradation using multi substrate degradation data (reaction media with TCP, BPA and TCS) in batch. SBP concentrations are a) 4.39×10^{-9} M, b) 8.77×10^{-9} M, and c) 1.75×10^{-8} M. Model quality was evaluated using adjusted R^2, RMSE, and objective function (OF) values reported in Table 3.

single-substrate degradation at an SBP concentration of 1.75×10^{-8} M. However, TCS degradation was not complete, because of the greater complexity of this molecule. This agrees with previous results concerning the oxidation of TCS catalyzed by different enzymes.[14] These behaviors occur because of a possible competition between the pollutants.

It's worth noting that the pH of all runs was measured at the start and end of each reaction, and in all cases, the pH values were found to be close to 6, which is the pH of the MilliQ water that was used to prepare the solutions.

3.3 Model validation and parameter estimation for single substrates

As proposed in section 2, the system of differential-algebraic equations (DAE) was solved using MATLAB R2015a, specifically with the *ode15s* solver, which applies the backward differentiation formula (BDF) method.

The complete definition of the model requires estimating the degradation rate constants for the reactions, k_1, k_2, and k_3. To this end, an optimization algorithm was used to compare the model results with experimental data.

The quality of the kinetic model fits was evaluated using complementary statistical criteria, including the adjusted coefficient of determination (adjusted R^2), root mean squared error (RMSE), and the objective function (OF) values obtained from weighted least squares minimization. Although adjusted R^2 provides a general indication of model performance, it is not always sufficient for assessing nonlinear kinetic models with multiple parameters. For this reason, RMSE and OF values were used in conjunction with adjusted R^2 to ensure a robust comparison between single- and multi-substrate models. The combined statistical analysis demonstrates that the multi-substrate kinetic model provides a superior description of the experimental data, particularly under conditions where substrate competition occurs.

Table 2 displays the estimated parameters and model fit evaluation for the degradation of a single substrate, and Fig. 5 depicts the model prediction and experimental data for these cases. To enable comparison with the multi-substrate model, the simplest model was considered, with the formation of only CpI and CpII. The multi-substrate model has more substrates and therefore more parameters. These results show that the single-substrate model accurately represented the data, with an adjusted R^2 always greater than 90%, except for the first set of TCS degradation experiments which had an adjusted R^2 of 64.65%.

3.4 Model validation and parameter estimation for multiple substrates

To simulate the multi-substrate degradation reactions, the estimated parameters obtained from the single-substrate degradation data were used first. The results of these simulations are presented in Table 3 and Fig. 6.

It has been noted that the single-substrate model is inadequate for accurately representing the degradation data of multiple substrates, particularly in cases such as TCP and TCS (Fig. 6). This simulation can serve as a reference point for comparing the results of parameter estimation obtained using the multi-substrate model. These results are presented in Table 4 and Fig. 7.

The results indicate that the multi-substrate model provides a more accurate representation of the substrate degradation data. This evidence is significant as the modified bi–bi ping pong model-based multi-substrate model is being proposed in this work.

Table 4 Estimated parameters and model fit evaluation for multi-substrate degradation in a reaction medium with TCP (A), BPA (B), and TCS (C)

Parameter	Value	Unit
k_1	2.0×10^7	$M^{-1}\ s^{-1}$
k_{2A}	1.12×10^6	$M^{-1}\ s^{-1}$
k_{3A}	9.80×10^4	$M^{-1}\ s^{-1}$
k_{2B}	1.21×10^6	$M^{-1}\ s^{-1}$
k_{3B}	5.36×10^5	$M^{-1}\ s^{-1}$
k_{2C}	1.63×10^6	$M^{-1}\ s^{-1}$
k_{3C}	1.16×10^4	$M^{-1}\ s^{-1}$
OF	7.3492×10^{-2}	—
RMSE	2.64×10^{-12}	—
$R^2_{\text{adjusted},1}$	96.47%	—
$R^2_{\text{adjusted},2}$	98.59%	—
$R^2_{\text{adjusted},3}$	98.51%	—

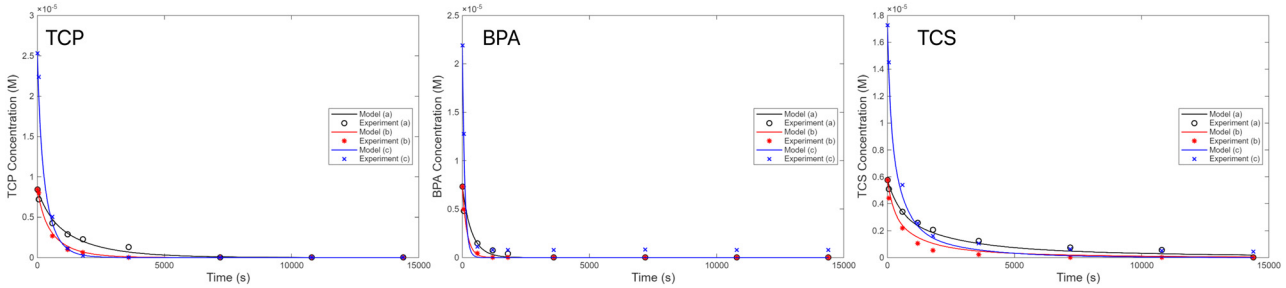

Fig. 7 Model prediction and experimental data of TCP (I), BPA (II) and TCS (III) multi-substrate degradation with SBP in batch. SBP concentrations are a) 4.39×10^{-9} M, b) 8.77×10^{-9} M, and c) 1.75×10^{-8} M. Model quality was evaluated using adjusted R^2, RMSE, and objective function (OF) values reported in Table 4.

While the single-substrate model provided a good fit for individual substrates, with an adjusted R^2 above 90% in most cases, it struggled to account for interactions in multi-substrate systems. In contrast, the multi-substrate model, with its ability to account for these interactions through additional parameters, captured the dynamics of simultaneous degradation processes, as shown by improved adjusted R^2 values and better alignment with experimental data in Fig. 7.

While the single-substrate model provided a good fit for individual substrates, with an adjusted R^2 above 90% in most cases, it struggled to account for interactions in multi-substrate systems. In contrast, the multi-substrate model, with its ability to account for these interactions through additional parameters, captured the dynamics of simultaneous degradation processes, as shown by improved adjusted R^2 values and better alignment with experimental data in Fig. 7.

This improved performance highlights the suitability of the model for real-world scenarios where pollutants often coexist, offering a more reliable tool for predicting degradation behavior in industrial applications.

The performance of the SBP enzyme highlights its importance for industrial applications, as it demonstrated faster and more efficient degradation across a wider range of pollutants.

Conclusions

SBP extracted from soybean hulls was successfully obtained and showed an activity of 35 μmol min^{-1}, with a calculated enzyme concentration of 8.85×10^{-5} M in the purified stock solution. In batch experiments, SBP promoted the degradation of TCP, TCS, and BPA under mild conditions, and the results showed that substrate behavior differs significantly between single- and multi-substrate systems because of competitive interactions.

The proposed modified bi–bi ping-pong kinetic model successfully described SBP-catalysed oxidation in complex reaction media. While the single-substrate model represented isolated reactions reasonably well, it was not able to capture the competitive effects observed in mixed systems. In contrast, the multi-substrate model reproduced the experimental concentration profiles more consistently, with improved statistical indicators, including adjusted R^2 values of 96.47–98.59% and RMSE of 2.64×10^{-12}.

Overall, this study provides quantitative kinetic insight into SBP-catalyzed degradation of TCP, TCS, and BPA in reaction media representative of complex effluents and delivers a useful reaction engineering framework for process modelling, reactor design, and future development of enzyme-based wastewater treatment systems.

Author contributions

Conceptualization: E. Laurenti, A. Vianna; investigation: A. S. da Cunha, M. Rigoletto; formal analysis: A. S. da Cunha; writing – draft: A. S. da Cunha; writing – review: A. S. da Cunha, M. Rigoletto, A. Vianna, E. Laurenti.

Conflicts of interest

There are no conflicts to declare.

Data availability

All data supporting the findings of this study are available within the article.

Acknowledgements

This study was financed in part by the Coordenação de Aperfeiçoamento de Pessoal de Nível Superior – Brasil (CAPES) – Finance Code 001. This paper is also part of a project that has received funding from the European Union's Horizon 2020 research and innovation programme under the Marie Skłodowska-Curie grant agreement no. 101007578 (SusWater). E. L. and M. R. acknowledge support from Project CH4.0 under MUR (Italian Ministry for the University) program "Dipartimenti di Eccellenza 2023-2027" (CUP: D13C22003520001).

References

1 G. Crini and E. Lichtfouse, *Environ. Chem. Lett.*, 2019, **17**, 145–155.

2 Y. Deng and R. Zhao, *Curr. Pollut. Rep.*, 2015, **1**, 167–176.
3 M. Rigoletto, E. Laurenti and M. L. Tummino, *Catalysts*, 2024, **14**, 42.
4 M. Nissum, C. B. Schiodt and K. G. Welinder, *Biochim. Biophys. Acta, Protein Struct. Mol. Enzymol.*, 2001, **1545**, 339–348.
5 M. M. Al Ansari, B. Saha, M. Samar, K. Taylor, J. Bewtra and N. Biswas, *Soybeans Cultiv. Uses Nutr.*, 2011, 189–221.
6 A. Steevensz, L. G. Cordova Villegas, W. Feng, K. E. Taylor, J. K. Bewtra and N. Biswas, *J. Environ. Eng. Sci.*, 2014, **9**, 181–186.
7 P. Calza, D. Zacchigna and E. Laurenti, *Environ. Sci. Pollut. Res.*, 2016, **23**, 23742–23749.
8 V. Tolardo, S. García-Ballesteros, L. Santos-Juanes, R. Vercher, A. M. Amat, A. Arques and E. Laurenti, *Water, Air, Soil Pollut.*, 2019, **230**, 140.
9 N. Caza, J. K. Bewtra, N. Biswas and K. E. Taylor, *Water Res.*, 1999, **33**, 3012–3018.
10 C. Watanabe, A. Kashiwada, K. Matsuda and K. Yamada, *Environ. Prog. Sustainable Energy*, 2011, **30**, 81–91.
11 J. Xiadong and H. Zheng, *Asian J. Chem.*, 2013, **25**, 5887–5890.
12 M. Rigoletto, P. Calza, A. S. da Cunha, V. Sederino, D. Fabbri, M. Laura Tummino and E. Laurenti, *React. Chem. Eng.*, 2023, **8**, 1629–1637.
13 T. P. Halappa Gowda, J. D. Lock and R. G. Kurtz, *Water, Air, Soil Pollut.*, 1985, **24**, 189–206.
14 J. Li, J. Peng, Y. Zhang, Y. Ji, H. Shi, L. Mao and S. Gao, *J. Hazard. Mater.*, 2016, **310**, 152–160.
15 K. Yamada, N. Ikeda, Y. Takano, A. Kashiwada, K. Matsuda and M. Hirata, *Environ. Technol.*, 2010, **31**, 243–256.
16 M. C. Silva, J. A. Torres, L. R. V. de Sa, P. M. B. Chagas, V. S. Ferreira-Leitao and A. D. Correa, *J. Mol. Catal. B:Enzym.*, 2013, **89**, 122–129.
17 L. Ai, T. Ren, Q. Yan, M. Wan, Y. Peng, X. Xu and X. Liu, *PLoS One*, 2021, **16**, e0257415.
18 *Biocatalysis Based on Heme Peroxidases*, ed. E. Torres and M. Ayala, Springer, Berlin, Heidelberg, 2010.
19 R. P. Ferrari, E. Laurenti and F. Trotta, *J. Biol. Inorg. Chem.*, 1999, **4**, 232–237.
20 E. Laurenti, E. Ghibaudi, G. Todaro and R. P. Ferrari, *J. Inorg. Biochem.*, 2002, **92**, 75–81.
21 E. Laurenti, E. Ghibaudi, S. Ardissone and R. P. Ferrari, *J. Inorg. Biochem.*, 2003, **95**, 171–176.
22 M. Bilal, D. Barceló and H. M. N. Iqbal, *Sci. Total Environ.*, 2020, **735**, 139194.
23 C. F. Melo and M. Dezotti, *J. Chem. Technol. Biotechnol.*, 2013, **88**, 930–936.
24 R.-N. Dou, J.-H. Wang, Y.-C. Chen and Y.-Y. Hu, *Environ. Pollut.*, 2018, **234**, 88–95.
25 L. Hong-Mei and J. A. Nicell, in *2011 International Conference on Multimedia Technology*, 2011, pp. 5442–5446.
26 I. Escalona, J. de Grooth, J. Font and K. Nijmeijer, *J. Membr. Sci.*, 2014, **468**, 192–201.
27 Q. Huang and W. J. Weber, *Environ. Sci. Technol.*, 2005, **39**, 6029–6036.
28 L. Hong-Mei and J. A. Nicell, *Bioresour. Technol.*, 2008, **99**, 4428–4437.
29 S. Kobayashi, H. Uyama, T. Ushiwata, T. Uchiyama, J. Sugihara and H. Kurioka, *Macromol. Chem. Phys.*, 1998, **199**, 777–782.
30 W. Zheng and L. M. Colosi, *Chemosphere*, 2011, **85**, 553–557.
31 Y. Zhang, M. Liu, J. Liu, X. Wang, C. Wang, W. Ai, S. Chen and H. Wang, *Environ. Toxicol. Pharmacol.*, 2018, **57**, 9–18.
32 M. Sarro, N. P. Gule, E. Laurenti, R. Gamberini, M. C. Paganini, P. E. Mallon and P. Calza, *Chem. Eng. J.*, 2018, **334**, 2530–2538.
33 M. Shintaku, K. Matsuura, S. Yoshioka, S. Takahashi, K. Ishimori and I. Morishima, *J. Biol. Chem.*, 2005, **280**, 40934–40938.
34 W. W. Cleland, *Nature*, 1963, **198**, 463–465.
35 J. G. Reich, *FEBS Lett.*, 1970, **9**, 245–251.
36 J. A. Nicell, *J. Chem. Technol. Biotechnol.*, 1994, **60**, 203–215.
37 J. A. Nicell and H. Wright, *Enzyme Microb. Technol.*, 1997, **21**, 302–310.
38 I. D. Buchanan and J. A. Nicell, *Biotechnol. Bioeng.*, 1997, **54**, 251–261.
39 R. A. Azizyan, A. E. Gevorgyan, E. S. Gevorgyan and V. B. Arakelyan, *Hayastani Kensabanakan Handes*, 2012, **2**, 85–93.
40 I. Durruty, E. Okada, J. F. González and S. E. Murialdo, *Biotechnol. Bioprocess Eng.*, 2011, **16**, 908–915.
41 M. Kong, Y. Zhang, Q. Li, R. Dong and H. Gao, *J. Microbiol. Biotechnol.*, 2017, **27**, 297–305.
42 R. A. Azizyan, A. E. Gevogyan, V. B. Arakelyan and E. S. Gevorgyan, *Int. J. Comput. Syst. Eng.*, 2013, **7**, 163–165.
43 J. L. Gómez, E. Gómez, J. Bastida, A. M. Hidalgo, M. Gómez and M. D. Murcia, *Chem. Eng. Process.*, 2008, **47**, 1786–1792.
44 J. L. Gómez Carrasco, E. Gomez Gomez, M. F. Máximo, M. Gomez Gomez, M. D. Murcia and S. Ortega Requena, *Chem. Eng. J.*, 2011, **166**, 693–703.
45 A. S. da Cunha, A. dos S. Vianna Jr. and E. Laurenti, *Braz. J. Chem. Eng.*, 2021, **2021**(38), 1–12.
46 T. T. Ngo and H. M. Lenhoff, *Anal. Biochem.*, 1980, **105**, 389–397.
47 J. K. A. Kamal and D. V. Behere, *Biochemistry*, 2002, **41**, 9034–9042.
48 R. A. Costa, A. S. Cunha, J. C. G. Peres, A. R. Azzoni, E. Laurenti and A. S. Vianna, *Symmetry*, 2020, **12**, 1129.
49 M. Schwaab and J. C. Pinto, *Análise de Dados Experimentais: I. Fundamentos de Estatística e Estimação de Parâmetros*, Servicoes Editoriales Ltda., 1st edn, 2007.

